

## Development of a Low-Profile Broadband Cavity Backed Bow-Tie Shaped Slot Antenna in SIW Technology

Bollavathi Lokeshwar<sup>1, \*</sup>, Dorai Venkatasekhar<sup>2</sup>, and Jammalamadugu Ravindranadh<sup>3</sup>

**Abstract**—A new design of broadband cavity-backed slot antenna (CBSA) based on substrate integrated waveguide (SIW) technology is presented in this paper. An entire proposed antenna is printed on a Rogers RT/Duroid 5870 substrate, which consists of the SIW cavity, bow-tie slot, microstrip line feed. The proper position and size of the bow-tie slot on top of the SIW cavity will generate the cavity modes, which can be merged to obtain the broadband response. Moreover, to understand the effects of the geometric dimensions of the broadband antenna on  $S_{11}$  are examined using parametric study. The final antenna configuration operates on a frequency band ranging from 9.25 GHz to 10.5 GHz with a fractional bandwidth of about 12.65% for the simulation part. The measured bandwidth for  $S_{11}$  is about 12.1% (9.3 GHz to 10.5 GHz). The proposed antenna has a good measured gain of 6 dBi and 6.6 dBi, at 9.55 GHz and 10.35 GHz, respectively. The gain, the reflection coefficient, and the radiation patterns of the fabricated antenna are measured and indicated a very good agreement with simulations.

### 1. INTRODUCTION

Microstrip slot antennas with light-weight, low-cost fabrication and ease of integration with printed circuit board designs are widely used, in applications such as electronic warfare, radar, mobile and satellite systems [1–3]. However, most of the slot antennas exhibit bidirectional radiation, and typically a metallic cavity must be used in order to eliminate back radiation [4]. However, these antennas are difficult to fabricate and integrate, bulky, and costly. Moreover, bandwidth limitation was observed due to the constraint on the height of the cavity [5, 6].

In recent times, a promising candidate, named ‘substrate integrated waveguide’ (SIW) technology, is introduced to design cavity backing structures for its outstanding benefits of easy integration, low power losses, huge power handling ability, and convenient fabrication using PCB technology [7, 8]. Therefore, the SIW exhibits the advantages of both microstrip line and metallic waveguide. Several designs of SIW CBSAs have been investigated for dual-band, polarization, size reduction in [9–12]. These designs retain advantages of low fabrication cost, low profile, and seamlessly planar integration. A circularly polarized SIW ring slot antenna [13] was proposed, whose impedance bandwidth was 10.3%, and axial ratio bandwidth was 2.3%.

In [14], the antenna exhibits an impedance bandwidth of 4.2% by employing offset feeding, instead of center feeding technique. In [15], a rectangle slot excites the two hybrid cavity modes to achieve a bandwidth of 6.3%. A SIW cavity-backed antenna [16] with two slots on the upper portion of the cavity shows a broadband response of 8% bandwidth. In [17], bilateral slots backed by a SIW cavity achieves an impedance bandwidth of 8.6%. In [18], a rectangle slot is replaced with a bow-tie slot, which further extends the bandwidth up to 9.4%. In [19],  $TM_{010}$  mode of the patch is excited through proximity

---

Received 24 July 2021, Accepted 20 August 2021, Scheduled 26 August 2021

\* Corresponding author: Bollavathi Lokeshwar (lokesh5701@gmail.com).

<sup>1</sup> Department of ECE, Annamalai University, Annamalainagar, India. <sup>2</sup> Department of IT, Annamalai University, Annamalainagar, India. <sup>3</sup> Department of ECE, R.V.R & J.C College of Engineering, Guntur, India.

coupling to improve the impedance bandwidth up to 10%. In [20], rectangle and triangular ring slots both excite the hybrid modes to achieve an impedance bandwidth up to 11%.

In this article, a CBSA using SIW technology is proposed for obtaining a wideband response. The antenna bandwidth is greatly influenced by the dimensions of the slot as well as the height of the substrate. In order to enhance the bandwidth, the SIW cavity of height about 1.6 mm is loaded, with a bow-tie shaped slot, which is a good antenna element for wideband application. The bow-tie slot antenna achieves 12.65% bandwidth with a  $25^\circ$  extended angle, which is a quite different approach. The measured findings are compared with the previously reported works for a more extensive study.

## 2. ANTENNA CONFIGURATION AND PROCEDURE

The structure of the proposed design and its parameters are shown in Figure 1. The proposed antenna is designed on a dielectric substrate with a height of 1.6 mm and a permittivity of 2.2. The proposed antenna consists of a SIW cavity ( $L \times W$ ), a bow-tie slot, and a microstrip line feed ( $L_f \times W_f$ ). The SIW cavity is built on a same substrate, where multiple plated through holes are connected with the top and bottom metal layers and penetrate through the dielectric layer. The slot has a length of half wavelength at the resonant frequency, which is printed on the top metal plate of the substrate and acts as a radiator. The size of the antenna is  $29.7 \text{ mm} \times 22 \text{ mm} \times 1.6 \text{ mm}$ .

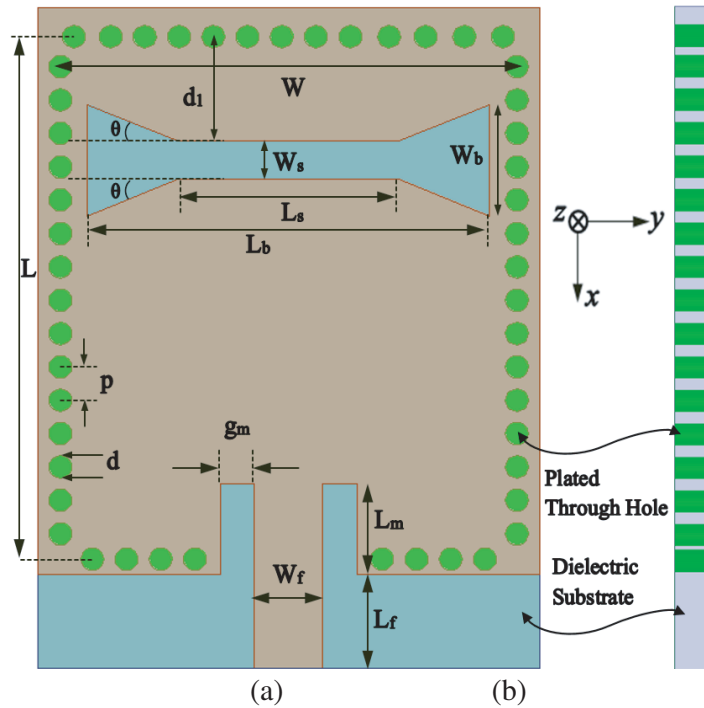


**Figure 1.** Structural representation of the antenna. (a) Schematic. (b) Side view.

To support the  $TE_{110}$  and  $TE_{210}$  modes, the SIW cavity dimensions are estimated by using the formula given in Equation (1). The length  $L$  of the rectangle cavity surrounded by plated through hole is 23.5 mm, and width  $W$  is 20 mm. The diameter of plated through hole is  $d = 1.0 \text{ mm}$ , and adjacent plated through hole center spacing is  $p = 1.5 \text{ mm}$ . In order to reduce the leakage losses, between adjacent plated through holes, values ' $d$ ' and ' $p$ ' are chosen in such a way that they must obey the rules of  $p/d \leq 2$  and  $d/\lambda_0 \leq 0.1$  [17]. Due to the discontinuity in plated through holes, the side wall current cannot flow longitudinally across the regular interval that stops the TM mode of propagation. The antenna is excited with a  $50 \Omega$  microstrip line. Table 1 lists the optimized parameters of the proposed

**Table 1.** Geometrical parameters.

Parameter	Value	Parameter	Value (mm)
$W$	20 mm	$g_m$	1.5 mm
$L$	23.5 mm	$W_s$	1.7 mm
$p$	1.5 mm	$L_s$	9.7 mm
$d$	1 mm	$W_b$	5 mm
$W_f$	3 mm	$L_b$	17.6 mm
$L_f$	4.2 mm	$d_1$	4.7 mm
$L_m$	4.1 mm	$\theta$	25°

design.

$$f_{mnp'} = \frac{1}{2\sqrt{\mu_0\epsilon_0\epsilon_r}} \sqrt{\left(\frac{m}{L_{eff}}\right)^2 + \left(\frac{n}{W_{eff}}\right)^2 + \left(\frac{p'}{h}\right)^2} \quad (1)$$

$$L_{eff} = L - \frac{d^2}{0.95 * p} \quad (2)$$

$$W_{eff} = W - \frac{d^2}{0.95 * p} \quad (3)$$

where  $m$ ,  $n$ , and  $p'$  are non-negative integers;  $W$  is the SIW cavity width,  $L$  is the SIW cavity length;  $\epsilon_r$  is the relative permittivity of the dielectric substrate;  $p$  is the pitch;  $d$  is the cylinder diameter.

### 3. WORKING MECHANISM

#### 3.1. Operating Principle

Simulation of the designed antenna is carried out by using ANSYS HFSS. SIW cavity is stimulated by microstrip line, at first, and it can be identified that the  $TE_{210}$  mode is generated, at 10 GHz. A

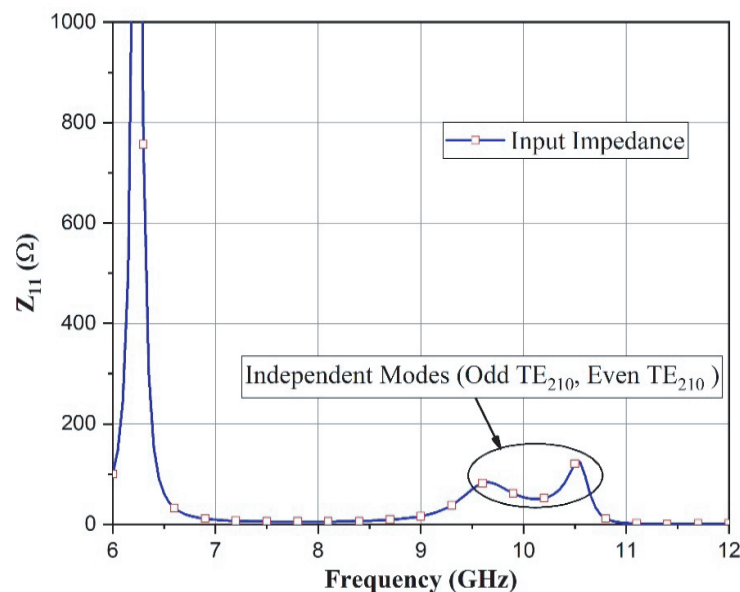


**Figure 2.** Input impedance of the proposed design.

common approach to increase the operating bandwidth of cavity-backed antennas is to increase the height of the dielectric material. That is why a standard thickness  $h = 1.6$  mm is selected as substrate thickness. The bow-tie slot introduces a strong loading effect on the  $TE_{210}$  mode of the cavity, and as a result, two different modes get excited in the cavity in close proximity. By attuning these modes with antenna dimensional parameters, a broadband response is obtained in the X-band. Input impedance of the antenna is shown in Figure 2, where perturbed cavity modes are identified for  $TE_{210}$  mode.

### 3.2. Field Distributions

To gain a better understanding, the E-field distribution at  $TE_{210}$  mode, 10 GHz is shown in Figure 3(a). Moreover, the phenomena of perturbation of  $TE_{210}$  mode within the SIW cavity can be displayed in Figures 3(b)–(c) with the help of H-field distribution. It is observed that due to the reactive loading of slot, two resonances are generated nearby at  $f_1 = 9.5$  GHz and  $f_2 = 10.3$  GHz, respectively. Figure 3(b) shows H-field in the region surrounding the slot at 9.5 GHz, while Figure 3(c) represents the presence of strong H-field in the above portion of slot at 10.3 GHz. At  $f_1$  and  $f_2$ , the difference in magnitude and phase of the H-field on the opposite side of the slot helps it to radiate into the air.

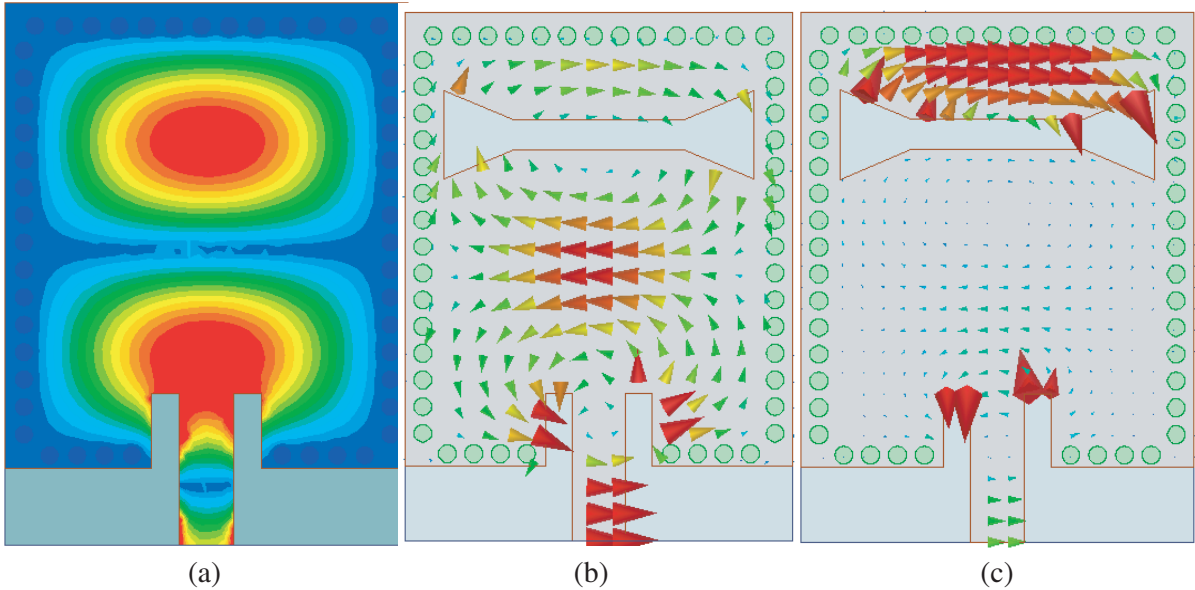


**Figure 3.** Field distributions. (a) E-field at 10 GHz. (b) H-field at 9.5 GHz. (c) H-field at 10.3 GHz.

### 3.3. Study of Different Parameters

To understand the working function of the proposed antenna, three parameters are selected to vary:  $W_s$  (width of middle rectangle slot),  $W_f$  (width of feed line), and  $d_1$  (position of the bow tie slot). During this analysis, when one of the parameters mentioned above is changed and the other parameters are kept as in Table 1, input impedance and impedance bandwidth gets affected. This parametric study demonstrates the useful information for optimizing the antenna parameters.

Figure 4(a) illustrates the simulated  $S_{11}$  (dB) versus frequency (GHz) for various values of width of the slot ( $W_s$ ). When the slot width is changed from 1.5 mm to 1.9 mm, it is noted that the lower resonances move up considerably, while the upper frequencies also move up slightly. Additionally, a larger  $W_s$  deteriorates the impedance bandwidth in the entire operating band. Thus, the good impedance matching is achieved at  $W_s = 1.7$  mm. In other words, ' $W_s$ ' strongly influences impedance matching of the antenna. A comparison between the different values of  $W_s$  is shown in Table 2. Figure 4(b) illustrates the simulated  $S_{11}$  of the antenna with different dimensions of the feed width, denoted as  $W_f$ . The simulation results indicate that the lower resonance shifts towards the upper side

**Table 2.** A comparison between the different values of  $W_s$ .

Variable parameter ( $W_s$ ) (mm)	Lower resonance ( $f_1$ ) (GHz)	Upper resonance ( $f_2$ ) (GHz)	$S_{11}$ (dB) at $f_1$	$S_{11}$ (dB) at $f_2$	Bandwidth (GHz)	Fractional Bandwidth (%)
1.5	9.45	10.3	-32.8	-19.5	9.25 to 10.35	11.22
1.7	9.55	10.35	-22.4	-26.9	9.30 to 10.50	12.12
1.9	9.65	10.45	-17	-17	9.40 to 10.50	11.05

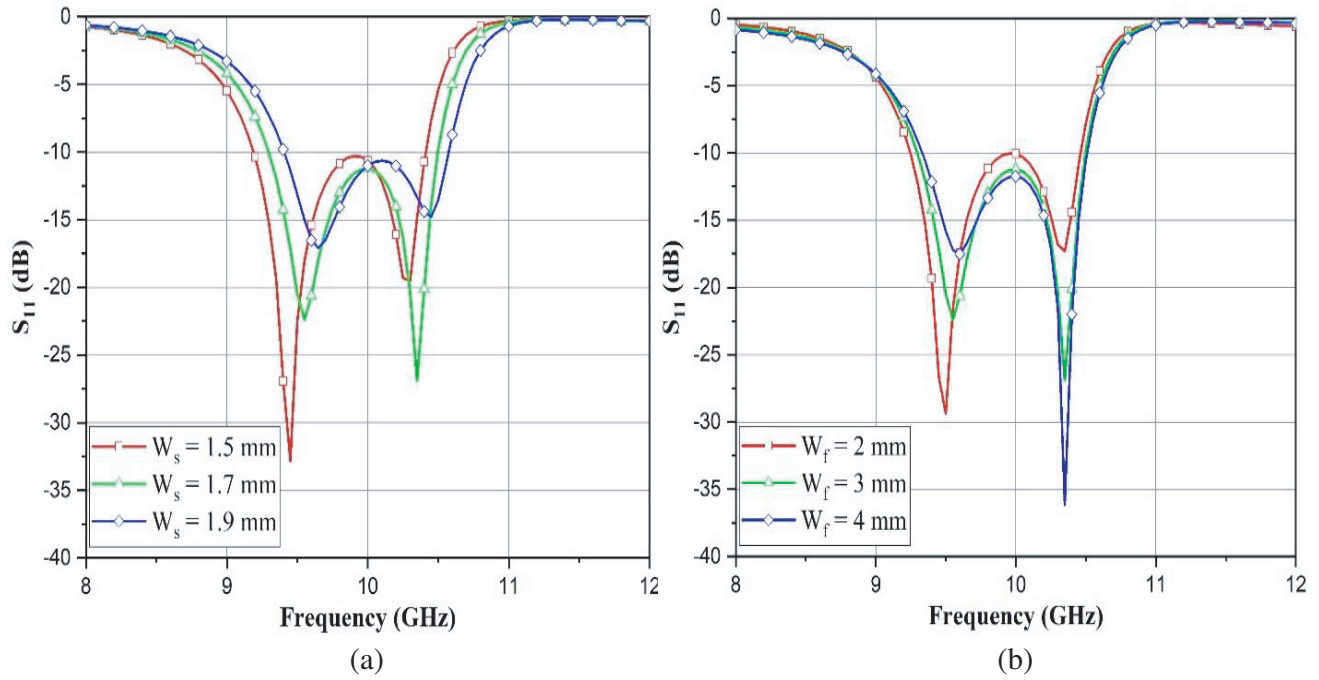


**Figure 4.** Simulated  $S_{11}$  in dB for various (a) slot width ( $W_s$ ), (b) feed width ( $W_f$ ).

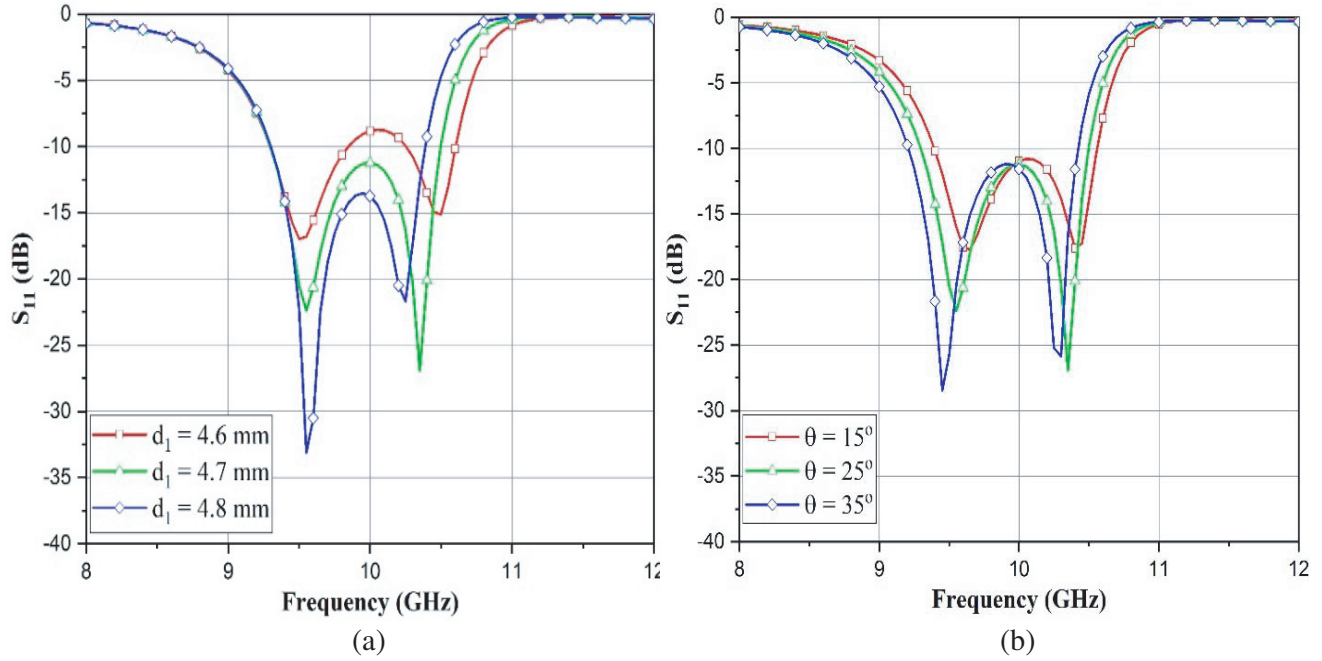
as  $W_f$  increases. Therefore, the antenna exhibits wideband response with the optimized dimension of 3 mm.

Figure 5(a) depicts the simulated  $S_{11}$  of the antenna for various values of slot position  $d_1$ , where the position of the slot shows a significant influence on the antenna performance as well as on the impedance matching. Therefore,  $d_1$  is chosen to be 4.7 mm for good fractional bandwidth. Figure 5(b) shows that when the extended angle  $\theta$  is varied, the two resonances are shifted toward a lower side. A comparison between the different values of  $\theta$  is shown in Table 3. With an increase in angle,  $S_{11}$

**Table 3.** A comparison between the different values of  $\theta$ .

Extended angle ( $\theta$ )	$S_{11}$ (dB) at $f_1$	$S_{11}$ (dB) at $f_2$	Bandwidth (GHz)	FTBR (dB)	Co-pol (dB)		X-pol (dB)	
					at $f_1$	at $f_2$	at $f_1$	at $f_2$
15	-17.5	-17.5	9.4 to 10.5 (1.1)	16.1	5.89	6.61	-33	-29
25	-21.5	-24	9.25 to 10.5 (1.25)	16.2	5.85	6.6	-32.6	-31
30	-28.4	-25.8	9.2 to 10.4 (1.2)	15.8	6	6.6	-31	-31

increases. So, broadband response is achieved at an optimum value of  $25^\circ$  in bow-tie slot antenna. This is a quite different approach as compared to conventional SIW cavity-backed slot antennas. Therefore, it is concluded that the changes in the dimensions will reduce the quality factor of the resonances, and as a result, bandwidth of the antenna gets improved.



**Figure 5.** Simulated  $S_{11}$  in dB for various (a) slot position ( $d_1$ ), (b) extended angle ( $\theta$ ).

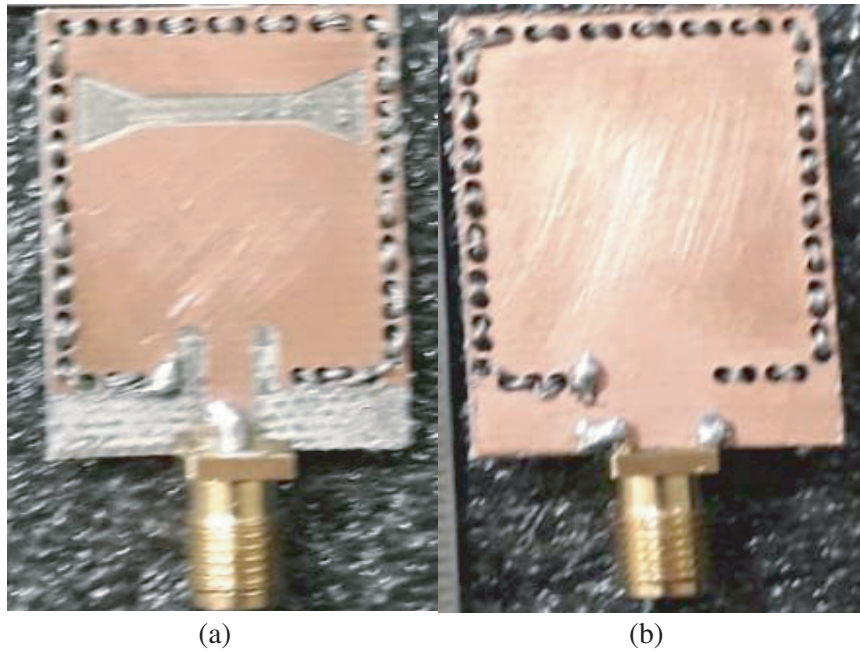


**Figure 6.** Fabricated prototype. (a) Top view. (b) Rear view.

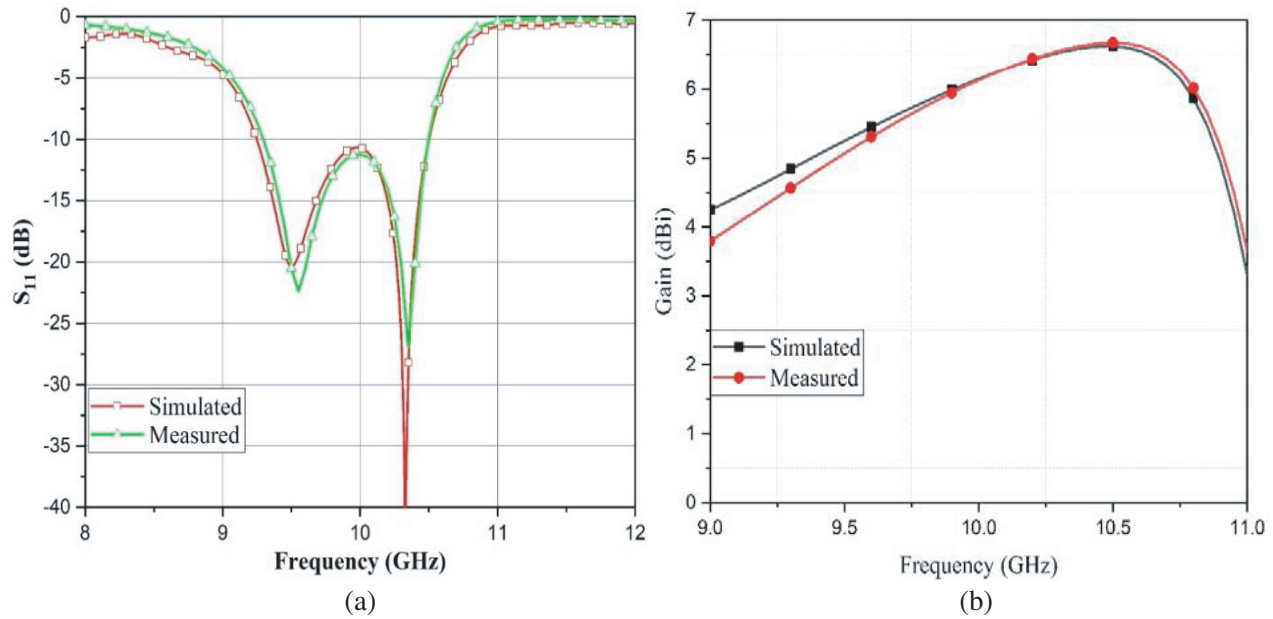


Figure 7. (a) Simulated and measured  $S_{11}$ . (b) Gain.

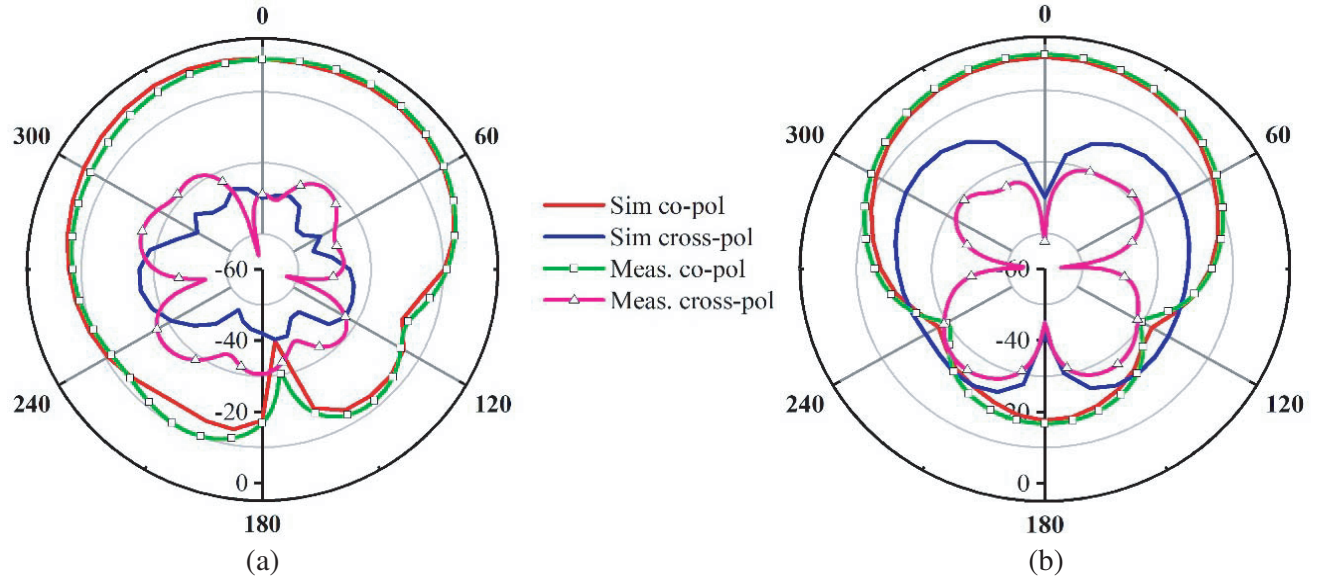
#### 4. RESULTS AND DISCUSSION

A prototype of the antenna is fabricated on an RT/Duroid 5880 substrate. To validate the simulated properties like return loss, gain, and radiation pattern, the fabricated sample is tested and verified practically. Figure 6 shows the photographs of the top and rear views of the fabricated sample. Figure 7(a) presents the simulated and measured  $S_{11}$  versus frequency, where the simulated bandwidth of  $-10$  dB return loss is 12.65%, and the measured bandwidth is 12.1%. Thus, it can be observed that the measured results are almost the same as the simulated ones. If at all, there is a small deviation, it may be because tolerances in fabrication and soldering, dielectric and conductor losses, and SMA connector effects. The graph of the measured gain is depicted in Figure 7(b). The proposed antenna shows peak gains of 6 dB and 6.6 dB, at 9.55 GHz and 10.35 GHz, respectively.

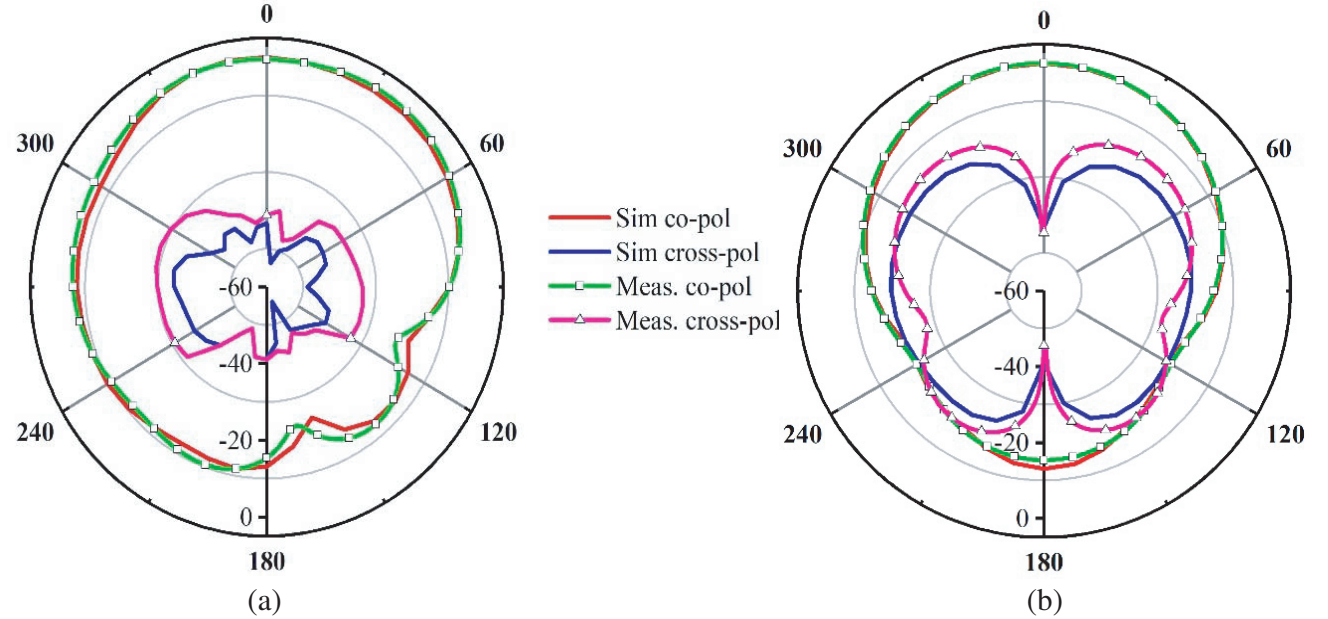
The normalized radiation patterns at 9.55 GHz and 10.35 GHz are shown in Figures 8 and 9, respectively. The radiation pattern of  $XZ$ - and  $YZ$ -planes at both the bands are corresponding to the  $E$ - and  $H$ -planes, respectively. The major lobe is always fixed in the broadside  $z$ -direction. It is caused by the introduction of the cavity-backing structure, which can reinforce the radiating energy in the  $z$ -direction and eliminate it in the back side. The peak CPL is below  $-20$  dB in the boresight direction, and the FTBR is about 14 dB. To highlight the essence of the proposed study, a comparison of different parameters of the proposed work with already published antennas in the X-band is listed in Table 4.

Table 4. Performance comparison: Proposed antenna with other designs.

References	Properties	Frequency band	FBW (%)	Gain (dBi)	$\epsilon_r$	Feed type
[14]		X	4.2	5.6	2.2	Microstrip
[15]		X	6.3	6	2.2	Microstrip
[16]		X	8	7.9	2.2	Microstrip
[17]		X	8.6	6.75	2.2	Microstrip
[18]		X	9.4	3.7	2.2	Microstrip
Proposed		X	12.1	6.6	2.2	Microstrip



**Figure 8.** Radiation patterns at 9.55 GHz. (a)  $E$ -plane ( $\phi = 0^\circ$ ). (b)  $H$ -plane ( $\phi = 90^\circ$ ).



**Figure 9.** Radiation patterns at 10.35 GHz. (a)  $E$ -plane ( $\phi = 0^\circ$ ). (b)  $H$ -plane ( $\phi = 90^\circ$ ).

## 5. CONCLUSION

This paper presents the design of a SIW cavity-backed antenna with a bow-tie shaped slot for X-band applications. A bow-tie slot placed at an appropriate position on the upper portion of a SIW cavity leads to bandwidth enlargement effectively. Moreover, the radiating slot perturbs the  $TE_{210}$  to enhance the bandwidth. The proposed antenna renders a measured bandwidth of 12.1 % and a gain of more than 6 dBi. It also substantiates a very good agreement between simulation and measured counterparts with respect to radiation behavior. The proposed design also exhibits light-weight, low-cost fabrication, and easy integration with planar circuits.



## REFERENCES

1. Yoshimura, Y., "A microstrip slot antenna," *IEEE Trans. Microw. Theory Tech.*, Vol. 20, No. 11, 760–762, 1972.
2. Huang, J. F. and C. W. Kuo, "CPW fed bow-tie slot antenna," *Microw. Opt. Technol. Lett.*, Vol. 19, No. 5, 358–360, 1998.
3. Locker, C., T. Vaupel, and T. F. Eibert, "Radiation efficient unidirectional low-profile slot antenna element for X-band application," *IEEE Trans. Antennas Propag.*, Vol. 53, No. 8, 2765–2768, 2005.
4. Harikowa, J., H. Arai, and N. Goto, "Cavity-backed wide slot antenna," *IEE Proceedings H — Microw. Antennas Propag.*, Vol. 136, No. 1, 29–33, 1989.
5. Zhou, S. G., G. L. Huang, and T. H. Chio, "A low profile wideband cavity-backed bowtie antenna," *Microw. Opt. Technol. Lett.*, Vol. 55, No. 6, 1422–1426, 2013.
6. Basit, M. A., G. Wen, R. Nouman, and X. Xue, "A wide-band cavity-backed slot antenna for end-fire radiation," *Microwave & Optical Tech. Letters*, Vol. 58, No. 1, 193–196, 2016.
7. Uchimura, H., T. Takenoshita, and M. Fujii, "Development of a laminated waveguide," *IEEE Trans. Microw. Theory Tech.*, Vol. 46, No. 12, 2438–2443, 1998.
8. Bozzi, M., A. Geordiadis, and K. Wu, "Review of substrate-integrated waveguide circuits and antennas," *IET Microw. Antennas Propag.*, Vol. 5, No. 8, 909–920, 2011.
9. Lokeshwar, B., D. Venkatasekhar, and A. Sudhakar, "Dual-band low profile SIW cavity-backed antenna by using bilateral slots," *Progress In Electromagnetics Research C*, Vol. 100, 263–273, 2020.
10. Luo, G. Q., Z. F. Hu, Y. Liang, L. Y. Yu, and L. L. Sun, "Development of low profile cavity backed crossed slot antennas for planar integration," *IEEE Trans. Antennas Propag.*, Vol. 57, No. 10, 2972–2979, 2009.
11. Bollavathi, L., V. Dorai, and S. Alapati, "Wideband planar substrate integrated waveguide cavity-backed amended dumbbell-shaped slot antenna," *AEU — International Journal of Electronics and Communications*, Vol. 127, 153489, 2020.
12. Dokuparthi, J. and A. Sudhakar, "Dual band half mode SIW semicircular cavity back slot antenna," *Progress In Electromagnetics Research Letters*, Vol. 87, 7–14, 2019.
13. Lacik, J., "Circularly polarized SIW square ring-slot antenna for X-band applications," *Microwave & Optical Tech. Letters*, Vol. 54, No. 11, 2590–2594, 2012.
14. Mukherjee, S., A. Biswas, and K. V. Srivastava, "Bandwidth enhancement of substrate integrated waveguide cavity backed slot antenna by offset feeding technique," *IEEE Applied Electromagnetics Conf. (AEMC)*, Dec. 2013.
15. Luo, G. Q., Z. F. Hu, W. J. Li, X. H. Zhang, L. L. Sun, and J. F. Zheng, "Bandwidth-enhanced low-profile cavity-backed slot antenna by using hybrid SIW cavity modes," *IEEE Trans. Antennas Propag.*, Vol. 60, No. 4, 1698–1704, 2012.
16. Varnoosfadetrani, M. V., J. Lu, and B. Zhu, "Matching slot role in bandwidth enhancement of SIW cavity-backed slot antenna," *Asia-Pacific Conf. on Antennas and Propag.*, 244–247, 2014.
17. Lokeshwar, B., D. Venkatasekhar, and A. Sudhakar, "Wideband low-profile SIW cavity-backed antenna bilateral slots antenna for X-band application," *Progress In Electromagnetic Research M*, Vol. 97, 157–166, 2020.
18. Mukherjee, S., A. Biswas, and K. V. Srivastava, "Broadband substrate integrated waveguide cavity-backed bow-tie slot antenna," *IEEE Antennas and Wireless Propagation Letters*, Vol. 13, 1152–1155, 2014.
19. Dashti, H. and M. H. Neshati, "Development of low profile patch and semi-circular SIW cavity hybrid antennas," *IEEE Trans. Antennas Propag.*, Vol. 69, No. 9, 4481–4488, 2014.
20. Kumar, A. and S. Raghavan, "Wideband slotted substrate integrated waveguide cavity-backed antenna for Ku-band application," *Microwave & Optical Tech. Letters*, Vol. 59, 1613–1619, 2017.